Modeling multiple time scale firing rate adaptation in a neural network of local field potentials

Brian Nils Lundstrom

Abstract In response to stimulus changes, the firing rates of many neurons adapt, such that stimulus change is emphasized. Previous work has emphasized that rate adaptation can span a wide range of time scales and produce time scale invariant power law adaptation. However, neuronal rate adaptation is typically modeled using single time scale dynamics, and constructing a conductance-based model with arbitrary adaptation dynamics is nontrivial. Here, a modeling approach is developed in which firing rate adaptation, or spike frequency adaptation, can be understood as a filtering of slow stimulus statistics. Adaptation dynamics are modeled by a stimulus filter, and quantified by measuring the phase leads of the firing rate in response to varying input frequencies. Arbitrary adaptation dynamics are approximated by a set of weighted exponentials with parameters obtained by fitting to a desired filter. With this approach it is straightforward to assess the effect of multiple time scale adaptation dynamics on neural networks. To demonstrate this, single time scale and power law adaptation were added to a network model of local field potentials. Rate adaptation enhanced the slow oscillations of the network and flattened the output power spectrum, dampening intrinsic network frequencies. Thus, rate adaptation may play an important role in network dynamics.

Keywords Neural networks · Rate adaptation · Local field potentials · Slow oscillations · Multiple time scale

B. N. Lundstrom (✉)
Department of Neurology, University of Washington, Seattle,
WA 98195, USA
e-mail: lundbr@uw.edu

1 Introduction

The firing rates of many single neurons adapt (Koch 1999, Dayan and Abbott 2001, Gerstner and Kistler 2002, Trappenberg 2002). For example, when the neuronal stimulus is suddenly increased, the rate of action potentials increases suddenly and then slowly decreases towards an apparent steady state, a phenomenon termed firing rate adaptation or spike frequency adaptation, first described over 75 years ago (Adrian and Zotterman 1926). Firing rate adaptation is often quantified by a gain parameter, the difference between the initial and apparent steady state responses, and a time scale, a description of the time course of the firing rate change.

How the adaptation time scale varies with different stimuli is key to understanding the dynamics and function of rate adaptation over a broad range of stimuli. Evidence suggests that adaptive processes of the neuron can modify firing rates over time scales ranging from tens of milliseconds to tens of seconds (Schwindt et al. 1988, Fleidervish et al. 1996, Abel et al. 2004, La Camera et al. 2006) and are implicated in single neuron adaptation to stimulus statistics (Sanchez-Vives et al. 2000, Higgs et al. 2006), which may serve to maintain maximal information transmission between stimulus and response (Barlow 1961, Brenner et al. 2000, Fairhall et al. 2001b). Other data from *in vitro* neocortical neurons (Lundstrom et al. 2008a) as well as *in vivo* neocortical and thalamic neurons (Lundstrom et al. 2010) demonstrate the presence of time scale invariant rate adaptation, such that the firing rate adapts via a power law process and is consistent with fractional differentiation of the input.

Rate adaptation emphasizes stimulus change and causes the phases of oscillations to advance, suggesting rate adaptation may promote information transmission or affect the synchronization of varying oscillations over neuronal populations (Wark et al. 2007, Lundstrom et al. 2008a, Pozzorini et al. 2013). Nonetheless, despite its observed prevalence in

neocortical neurons, rate adaptation lacks clear functional significance at the network or circuit level. Several factors may contribute to this. Conceptually the details of rate adaptation can be deceptively difficult to understand (Benda and Herz 2003), computational modeling of multiple time scale adaptation is nontrivial (Drew and Abbott 2006), and experimentally characterizing adaptation via single time scale exponential fitting is suboptimal (Fairhall et al. 2001a, Fairhall et al. 2001b, Lundstrom et al. 2008a). Previous rate models have typically been restricted to dynamics that are exponential in nature (La Camera et al. 2004). Implementing multiple time scale adaptation of a particular weighting in conductance-based models is difficult, as is assessing the effect of differing adaptation dynamics on neural networks.

Here, the intent is to describe an approach for modeling multiple time scale rate adaptation in a neural network and demonstrate its use in the Jansen and Rit model (Jansen and Rit 1995), a standard model of local field potentials (LFPs) that does not include rate adaptation. Adding rate adaptation to this model is motivated by the physiological importance of slow oscillations of LFPs (Steriade et al. 1993, Demanuele et al. 2013) and data implicating a related role for rate adaptation. Slow oscillations (~0.1-1 Hz) are sometimes parsed into Up and Down states (Steriade 2006), where rate adaptation is thought to play a role in the transitions (Destexhe et al. 2007). Large conductance-based models have demonstrated slow oscillations of ~0.1–0.4 Hz related to slow adaptation currents (Compte et al. 2003) and extrinsic stimuli (Lundqvist et al. 2013). Other evidence suggests that low levels of acetylcholine promote these slow rhythms and increase slow after-hyperpolarization potentials (Fellous and Sejnowski 2000), which underlie rate adaptation. The question is then whether the addition of rate adaptation to the Jansen and Rit model, a lumped parameter model of a single cortical column, can facilitate slow oscillations.

With the presented modeling approach, rate adaptation is modeled as a set of weighted exponential filters that act on slowly varying stimulus statistics and allow one to approximate adaptation of arbitrary dynamics. In this way, single time scale exponential adaptation and multiple time scale power law adaptation are added to the Jansen and Rit model (Jansen and Rit 1995). Results suggest that rate adaptation increases the effect that slow oscillation stimuli have on the network. In addition, power law adaptation flattens the output power spectrum, minimizing the effect of intrinsic oscillatory behavior from the network.

2 Methods

The Jansen and Rit model of local field potentials (Jansen and Rit 1995) is a lumped parameter model of a single cortical column comprised of pyramidal neurons as well as excitatory

and inhibitory interneurons. The model was implemented as a system of ordinary differential equations (ODEs), as previously (Jansen and Rit 1995, David and Friston 2003). To this system of differential equations, rate adaptation was added, which increased the number of equations in the system, as in the Appendix. For simplicity, the filter or integral equations of this model are referred to in Figs. 4 and 5, rather than the differential forms.

3 Results

3.1 Specifying a rate model with arbitrary adaptation time scales

An initial step to modeling multiple time scale rate adaptation is to model rate adaptation with a single filter that best describes the desired adaptation dynamics. Previous work demonstrates the general principle that rate adaptation is conceptually the difference between a non-adapted response and adaptive negative feedback (Ermentrout 1998, La Camera et al. 2004, Tripp and Eliasmith 2010). Benda and Herz (2003) show in detail that when the dynamics of rate adaptation are significantly slower than those of the spike generator, the details of spike generation are unimportant and the nonlinearities of the adapted firing rate response as a function of the stimulus are modest. In other words, a key insight is that the dynamics of spike generation, which are complicated, can be separated from the dynamics of adaptation, which are simpler and can be approximated in many cases as linear. Rate adaptation can act as a linear filter on slowly varying stimulus statistics, aside from a nonlinearity that ensures firing rates are non-negative.

In general, there are two forms the adaptation filter model can take, displayed here in both the time and frequency domains:

$$r = x - h * x \overset{F}{\longleftrightarrow} R = X - HX \tag{1}$$

and

$$r = h' * x \overset{F}{\longleftrightarrow} R = i\omega HX \tag{2}$$

where r is the rate response to a slowly time-varying stimulus x and filter h determines the nature of the adaptation feedback. The two forms highlight a point of nomenclature regarding adaptation dynamics, which can refer either to the dynamics of a hidden adaptation variable or the dynamics of the firing rate itself in response to a step stimulus. Specifically, in Eq. (1) the impulse response is $1-h(t)$, where the filter $h(t)$ specifies the dynamics of an implicit adaptation variable and the step response is only approximated by $h(t)$. In Eq. (2) the impulse

response is the derivative of the step response. In this case, the step response is specified precisely by $h(t)$, while the dynamics of feedback adaptation are only approximately $h(t)$. Implicit in the above forms is a nonlinear thresholding function that sets any negative firing rate values to zero. To be effective, this is a nonlinear function performed after adaptation filtering.

To be explicit, rate adaptation dynamics including a single exponential, the dynamics most commonly used, is demonstrated and the linear filter derived that represents single exponential adaptation. In its simplest form, rate adaptation can be viewed as the difference between an input and negative feedback (Benda and Herz 2003, La Camera et al. 2004, Tripp and Eliasmith 2010):

$$r = mx - ga$$
$$\frac{da}{dt} = \frac{-a}{\tau} + kr \tag{3}$$

where a is an adaptation variable with exponential kinetics, τ is the relaxation time constant of the adaptation variable, and m, g, and k are gain constants. In this context, the stimulus x is any slow time-varying component of the stimulus that positively affects the firing rate, such as the mean or standard deviation of the stimulus (Lundstrom et al. 2008a, Lundstrom et al. 2008b, Lundstrom et al. 2009). Faster time-varying stimulus components are effectively constant as the model implicitly assumes the effects of the spike generator can be averaged over several inter-spike intervals (Benda and Herz 2003). Expressed in the frequency domain, Eq. (3) becomes (Appendix):

$$R = m\left(\frac{1 - gk\tau_{eff} + i\omega\tau_{eff}}{1 + i\omega\tau_{eff}}\right)X = m\left(1 - \frac{gk\tau_{eff}}{1 + i\omega\tau_{eff}}\right)X \tag{4}$$

and as a single equation in the time domain:

$$r(t) = m\left(x(t) - gkx(t) * e^{-t/\tau_{eff}}\right)$$

where $0 \leq gk\tau_{eff} \leq 1$ and τ_{eff} is the effective time constant with $\tau_{eff} = (1/\tau + gk)^{-1}$ giving $\tau_{eff} \leq \tau$, a relationship referred to previously (Ermentrout 1998, Wang 1998, Tripp and Eliasmith 2010). This filter represents a high pass filtering system, with phases that lead the stimulus (Fig. 1), a property fundamental to rate adaptation (Appendix). The magnitude shows that low frequencies are attenuated, and in this case the phase advances to a maximum of approximately 20° at a period of 9 s (0.33 Hz). Increasing τ_{eff} leads to an increasing phase lead that peaks at a higher period, as does increasing gk, albeit with a weaker effect of shifting the maximal phase lead. Keeping
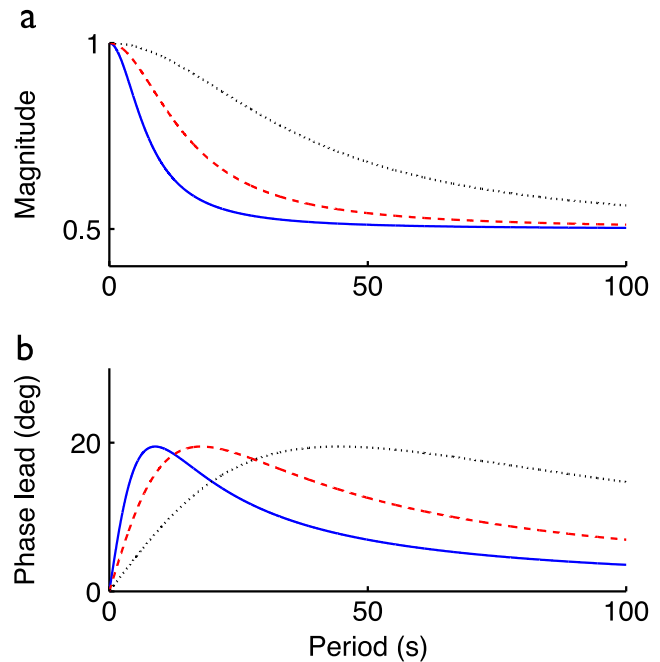
Fig. 1 The (**a**) magnitude and (**b**) phase responses as a function of period for Eq. (4) with $gk = [0.5\ 0.25\ 0.1]$ and $\tau_{eff} = [1\ 2\ 5]$ for the solid, dashed, and dotted lines, respectively. Gain $m = 1$

$gk\tau_{eff}$ fixed yields a constant maximal phase lead, which is proportional to the negative feedback exerted by the adaptation current.

Eq. (4) is an example of the first form of the adaptation model as in Eq. (1), where the adaptation variable a decays precisely as a single exponential as specified by $h(t)$, while the overall rate decay is approximately exponential, as noted previously (Liu and Wang 2001). This is in contrast to the second form of the rate adaptation model as in Eq. (2), shown below with dynamics of a single exponential. In this case, the adaptation filter $h(t)$ specifies precisely the dynamics of rate decay after a step increase of the input. Adaptation of the system is defined as the response of the system to a step increase, or Heaviside function, rather than an impulse function. The step function is the integral of the impulse, or delta, function (Harris and Stöcker 1998). Whereas $h(t)$ is typically the response of a system to the delta function, here h_{st} the response of the system to the step function stimulus $u(t)$ is needed:

$$h_{st}(t) = h*u(t) = h*\int\delta(t)dt = \int h(t)dt \tag{5}$$

where $\delta(t)$ is delta function. This gives:

$$h_{st} = \int h(t)dt \xrightarrow{F} H_{st} = \frac{1}{i\omega}H \tag{6}$$

where h_{st} and H_{st} are the system responses to a step function in the time and frequency domains, respectively. In other words,

the derivative of the step response gives the impulse response, and the second form of the adaptation filter model is:

$$r(t) = h_{st}'(t)*x(t) \xrightarrow{F} R(\omega) = i\omega H_{st}(\omega)X(\omega) \qquad (7)$$

where the step response dynamics are specified by h_{st}.

To see how the two forms compare, note that a response that decays as a single exponential has the form $1/(1+i\omega\tau)$ in the frequency domain:

$$H_{st} = \frac{c}{1 + i\omega\tau_{eff}} = \frac{1}{i\omega}H$$
$$R = \frac{i\omega c}{1 + i\omega\tau_{eff}}X = \left(1 - \frac{1 + i\omega\tau_{eff} - i\omega c}{1 + i\omega\tau_{eff}}\right)X \qquad (8)$$

where c is an arbitrary constant. Thus, the dynamics of adaptation differ depending on whether one refers t o the response to a step stimulus or to the dynamics of the adaptation variable. The two methods produce equivalent results when $k_1 h'(t) = k_2 - k_2 h(t)$, where k_1 and k_2 are constants, which gives a differential equation with solutions having the form of exponentials. In other words, to the degree that the filter $h(t)$ can be approximated by exponentials, these methods will be similar and give the approximate results mentioned above. This approach can similarly be used to directly model multiple time scale processes such as time invariant power law rate adaptation (Appendix).

3.2 Quantifying rate adaptation using phase leads of linear filters

By using the above filter models, specifying adaptation dynamics is equivalent to specifying the form of $h(t)$. However, not all forms of $h(t)$ are easy to implement, such as modeling power law adaptation in a neural network. One solution is to approximate the adaptation dynamics with a general model comprised only of exponential filters, and then fit the needed parameters by assessing adaptation via phase leads. One advantage to this approach is that the exponential filters preserve a correspondence with biophysical conductance-based channels, which themselves are characterized by a weight, or conductance, and a time scale (Hodgkin and Huxley 1952).

Rate adaptation has typically been quantified by examining the firing rate in response to a square wave pulse, such as by fitting exponential curves to the rate to find the amplitude and decay time constant (Liu and Wang 2001, La Camera et al. 2006). However, this can be imprecise when dealing with multiple time scale dynamics in the time domain (Lundstrom et al. 2008a). An alternative is to assess the phase responses of the neuron to varying input frequencies. In general, rate

adaptation gives rise to phase leads (Appendix), whereas rate facilitation produces phase lags. In the case of Eq. (4) $gk\tau$ is proportional to the amount of negative feedback provided by the adaptation current, which is quantified by measured phase leads. As an example, consider the firing rate response of a Hodgkin-Huxley (HH) conductance-based neuron with a slow potassium channel with exponential dynamics, simulated as previously (Lundstrom et al. 2008a). An increased time constant leads to greater phase advances and to phase advances at higher periods (Fig. 2).

A rate adaptation model comprised of exponential filters can be found by generalizing Eq. (3) to include multiple adaptation currents, expressed in the frequency domain as:

$$R(\omega) = mX(\omega) - \sum_n g_n A_n(\omega)$$
$$i\omega A_n(\omega) = -A_n(\omega)/\tau_n + kR(\omega) \qquad (9)$$

for n exponentially decaying currents with time constants τ_n, gain parameters g_n, and overall adaptation gain parameter k. This can be solved algebraically to find:

$$R(\omega) = H_{exp}X(\omega) = \frac{m}{1 + k\sum_n \dfrac{g_n}{1/\tau_n + i\omega}}X(\omega) \qquad (10)$$

which gives a general rate adaptation model with n exponentially-decaying adaption currents described by n gain and time constants.

To the extent that the details of the spike generator of conductance based models can be ignored (Benda and Herz 2003), Eq. (10) models the effect on rate of multiple adaptation currents, where each exponential filter can be mapped to a distinct adaptation current. Here, slow adaptation currents with different time scales can be thought of as multiple slow potassium after-hyperpolarization currents, which can be approximated as

$$I_n \propto g_n a_n \qquad (11)$$

where a_n is the adaptation variable time-averaged over the period of a typical interspike interval and g_n is proportional to the maximal conductance of the nth ion channel, with units of firing rate per unit of adaptation variable a.

One advantage of this formulation is that it allows for a quantitative assessment of adaptation via phase leads. Since this system with its filter H_{exp} is stable and causal, and since τ_n is always positive ensuring that all zeros are on the left side of the Laplace s-plane, the system is a minimum phase system (Ulrych and Lasserre 1966, Oppenheim et al. 1999), which

Fig. 2 Amount and time scale of rate adaptation is quantified by the peak and shift of the phase lead curve. (**a**) Hodgkin-Huxley neuron with a slow adaptation current with a time constant of 1 s (*solid*) and 6 s (*dashed*) adapts to a stimulus step increase. (**b**) Maximal phase lead increases as the adaptation current time constant increases
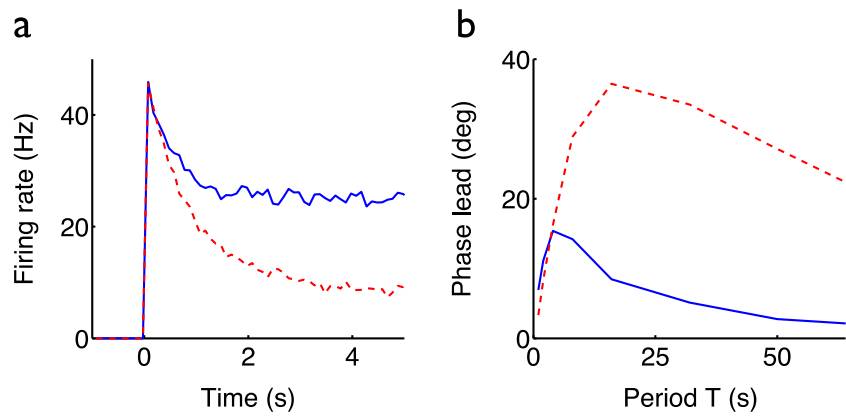
means that the phase and the magnitude of the system determine one another to within a multiplicative constant (Appendix). Knowledge of phase leads over varying input frequencies specifies the adaptation filter.

To implement power law adaptation in a network, H_{exp} is fitted such that it approximates power law adaptation. The power law filter H serves as a cost function to find the appropriate parameters for H_{exp}:

$$\min \sum \left| H(\omega) - H_{\exp}(\omega) \right| \qquad (12)$$

or via a cost function of the integrated squared error form, or other methods for frequency domain identification (Vinagre et al. 2000). For each of the n exponential filters in $H_{\exp}(\omega)$ there are two parameters g_n and τ_n, as well as the overall k parameter. Since $H_{\exp}(\omega)$ is a minimum phase system, one can minimize Eq. (12) with respect to only the phases of the filters, rather than the complete system function. This allows one to avoid specifying an overall gain for the adaptation filter $H(\omega)$, since the filter gain is arbitrary.

The chosen target filter of $H(\omega) = (i\omega)^{\alpha}$ is a power law adaptation filter for a fractional differentiator, which has been shown to approximate neocortical rate adaptation (Lundstrom et al. 2008a, Lundstrom et al. 2010). With $\alpha = 0.15$ this filter has a frequency-independent phase lead of about 13.5°, as seen in cortical slice experiments (Fig. 3a). To find $H_{exp}(\omega)$ three exponentials ($n = 3$) with $\tau = [0.3\ 1\ 6]$ sec are chosen; these time scales were used in prior work (Lundstrom et al. 2008a, Lundstrom et al. 2010) in order to span a range of adaptation time scales suggested by physiological data (Schwindt et al. 1988, Fleidervish et al. 1996, Abel et al. 2004). Minimizing over the phases of $H(\omega)$ and $H_{exp}(\omega)$ according to Eq. (12), gives the unique solution $kg_n = [1.23\ 0.23\ 0.14]$ Hz for the exponential filters of $H_{exp}(\omega)$ with $\tau = [0.3\ 1\ 6]$ sec. Previous work (Lundstrom et al. 2008a) used a conductance-based model with three slow potassium channels to approximate $H(\omega)$, where g_n were laboriously hand-tuned to approximate a near constant phase over frequencies $T = 1$–

50 s. In contrast, using the above fitting procedure the weighting of the time scales in $H_{exp}(\omega)$ are similar to previously (Fig. 3b) but found via a method suggesting a near optimal solution given the constraints.

3.3 Adding rate adaptation to a model of local field potentials

Rate adaptation is modeled as an adaptation filter comprised of a set of exponential filters, and this general adaptation model with three exponential filters has been fit to a power law filter such that it approximates power law adaptation. Rate adaptation can then be added to simplified neural networks, such as neural mass models (Wendling et al. 2000, Deco et al. 2008, Moran et al. 2013), and here it is added to a model of local field potentials.

The Jansen and Rit model of local field potentials (Jansen and Rit 1995) is a lumped parameter model, or neural mass model, of a single cortical column. The model is comprised of three neural populations: pyramidal neurons as well as excitatory and inhibitory interneurons (Fig. 4a). Each population is modeled by either an excitatory alpha synapse or an inhibitory alpha synapse that acts on synaptic inputs. The average post-synaptic membrane potential of the neural populations is transformed to an average pulse density of action potentials by a nonlinear sigmoid function, which serves primarily to rectify the signal. An external stimulus represents stimuli from other cortical columns as well as subcortical inputs. The three filter equations (Fig. 4a) can be implemented directly as integral equations or as a system of ordinary differential equations (ODEs) as previously (Jansen and Rit 1995, David and Friston 2003). The output of the model is the difference between the post-synaptic excitatory and inhibitory membrane potentials to the pyramidal neurons ($y_1 - y_2$), consistent with what is thought to primarily underlie the signal of electroencephalography (Nunez and Srinivasan 2006). The neural populations interact to produce intrinsic oscillations apart from any oscillatory stimulus (Fig. 4b), which is a general property of two neural populations with interacting excitatory and inhibitory neurons (Ermentrout and Cowan 1979). In this
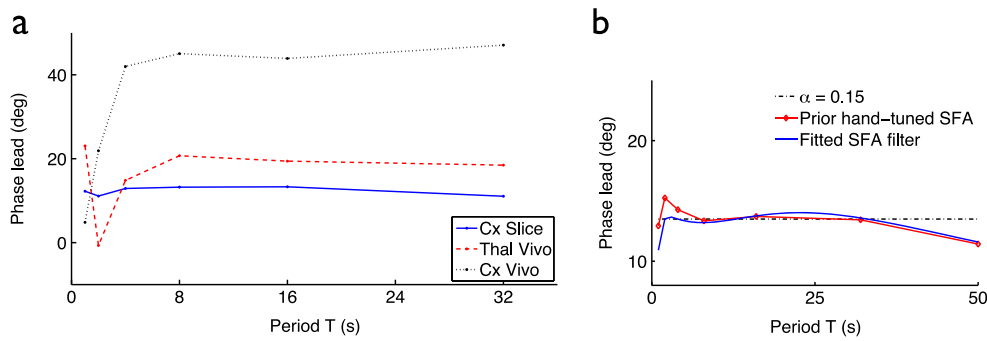
Fig. 3 a From previously published data, phase leads of firing rates for *in vitro* and *in vivo* neurons are consistent with multiple time scale processes, such as fractional differentiation (Lundstrom et al. 2008a, Lundstrom et al. 2010). Average response phase leads were statistically constant for *in vitro* cortical pyramidal neurons in response to sinusoidal time-varying currents (*solid*), and for *in vivo* thalamic neurons (*dashed*) and *in vivo* barrel cortex neurons (*dotted*) in response to sinusoidal whisker movements. **b** The phase as a function of period of a

conductance-based Hodgkin-Huxley model with hand-tuned conductances for three slow adaptation currents from prior work above is similar to that found by minimizing the exponential filter model (the fitted SFA filter). The fitted parameters were $kg_n=$ [1.23 0.23 0.14] Hz for the exponential filters of $H_{exp}(\omega)$ with $\tau=$[0.3 1 6] s while the parameters for the hand-tuned potassium conductances where $G=$ [1.5 0.18 0.12]/ 100 mS/cm^2 for the slow potassium channels with $\tau=$[0.3 1 6] s. The dashed line represents an ideal power law filter

model a wide variety of oscillatory outputs is possible depending on parameter choice (David and Friston 2003).

The Jansen and Rit model does not include any cell intrinsic rate adaptation, as the spike generation of the neural mass populations is represented solely by the nonlinear sigmoid function. Rate adaptation is added to the pyramidal population via the inclusion of an adaptation filter prior to the sigmoid nonlinearity of the pyramidal neuron (Fig. 5a). The

nonlinearity is sharp and effectively functions to rectify the output. That the adaptation filter is applied prior to rectification relates to the fact that while action potentials increase adaptation, adaptation currents reduce firing by acting on currents prior to spike generation (Hodgkin and Huxley 1952, Connor and Stevens 1971, Benda and Herz 2003). The nonlinearity comes after adaption filtering in order to effectively rectify the signal.
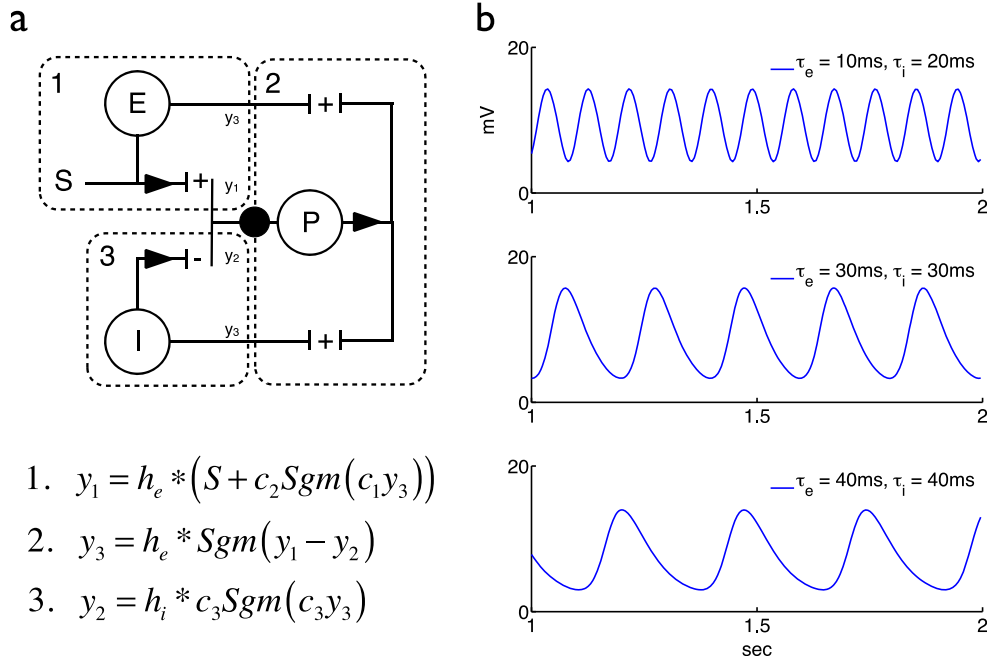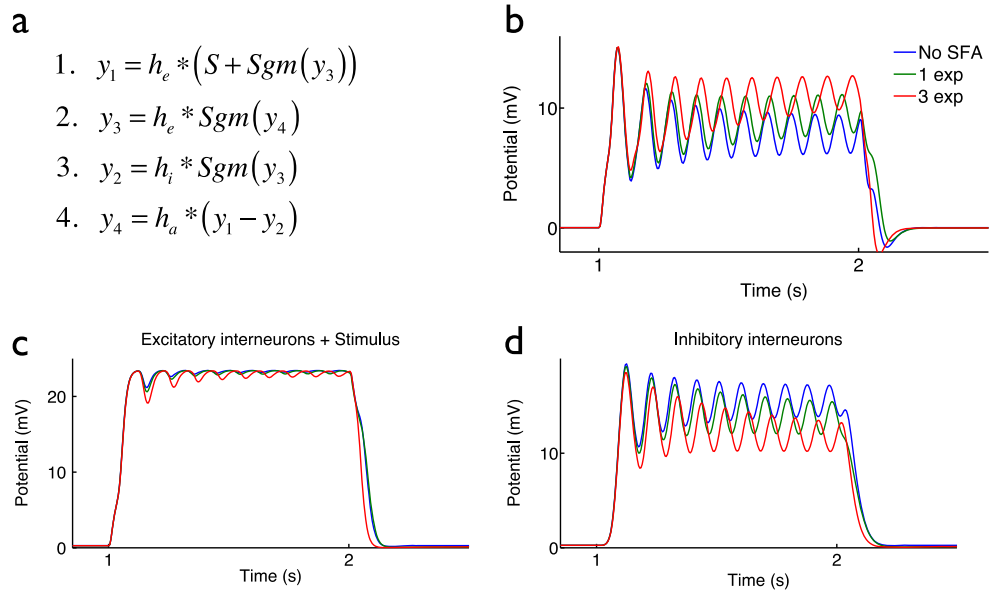

$$1. \quad y_1 = h_e * \left(S + c_2 Sgm(c_1 y_3) \right)$$

$$2. \quad y_3 = h_e * Sgm(y_1 - y_2)$$

$$3. \quad y_2 = h_i * c_3 Sgm(c_3 y_3)$$

Fig. 4 a Jansen and Rit neural mass model of brain activity with pyramidal neurons (P), excitatory interneurons (E), inhibitory interneurons (I), and an external stimulus (S). Model output (*solid black circle*) is the sum of excitatory and inhibitory synaptic inputs to the pyramidal neuron. Filters representing excitatory synapses $h_e= k_e/\tau_e t\, exp(-t/\tau_e)$ for $t \geq 0$ or inhibitory synapses $h_i= k_i/\tau_i t\, exp(-t/\tau_i)$ for $t \geq 0$ act on synaptic inputs. The nonlinear sigmoid function, $Sgm(v)= e_0/ [1+exp(0.56(6-v)]$,

transforms post-synaptic potentials. **b** For differing combinations of time constants, which govern synaptic filtering, the oscillation frequency of the model changes. Parameters are $k_e=40/\tau_e$ and $k_i=440/\tau_e$ with constant stimulus $S=400$Hz. Standard constants $c_{1-3}= [135\ 108\ 33.75]$ are obtained from prior data as previously (Jansen and Rit 1995) and are proportional to synapse number

Fig. 5 **a** Adaptation filter (h_a) is added as a fourth equation, simulating cell intrinsic rate adaptation of the pyramidal neurons. **b** Postsynaptic inputs to the pyramidal neurons (y_1– y_2) decrease in frequency in response to a constant boxcar stimulus ($S = 100$ Hz) when more rate adaptation is added. Models without spike frequency adaptation (SFA), with single time scale adaptation ($\tau = 1$ s), and with multiple time scale adaptation ($\tau = [0.3 \ 1 \ 6]$ s) are represented by *blue*, *green*, and *red* traces, respectively. **c** Post-synaptic excitatory inputs remain largely unchanged while **d** inhibition decreases with increased adaptation

a

$$1. \quad y_1 = h_e * \left(S + Sgm(y_3) \right)$$

$$2. \quad y_3 = h_e * Sgm(y_4)$$

$$3. \quad y_2 = h_i * Sgm(y_3)$$

$$4. \quad y_4 = h_a * (y_1 - y_2)$$

b

c Excitatory interneurons + Stimulus

d Inhibitory interneurons

Depending on the form of the adaptation filter h_a, arbitrary adaptation dynamics of any time scale can be implemented. Here, both single exponential dynamics and approximate power law adaptation are implemented. In the case of the single exponential adaptation, H_a is specified in Eq. (4) with $kg = 0.46$ Hz and $\tau = 1$ s. For approximate power law adaptation, H_a results from fitting, shown in Fig. 3b, which has the form of H as in Eq. (10) with three exponential filters and parameters $kg_n = [1.23 \ 0.23 \ 0.14]$ Hz with time constants chosen to be $\tau = [0.3 \ 1 \ 6]$ s.

In response to a sudden stimulus increase, or boxcar stimulus, the Jansen and Rit model with added rate adaptation shows increased slowing of the intrinsic oscillations as more adaptation is added to the model (Fig. 5b). Specifically, approximate power law adaptation shows more slowing than does single time scale adaptation, due to the presence of longer time scales. This effect is primarily due to reduced inhibition from decreased pyramidal output, since the post-synaptic inputs to the pyramidal neurons from the excitatory interneurons and stimulus (Fig. 5c) remains largely unchanged while inhibitory inputs decrease with increasing adaptation (Fig. 5d). Of note, without any added rate adaptation the model does display some features of adaptation, such as decreasing output amplitude over time (Fig. 5b, blue trace). This is related to the dynamics of the inhibitory and excitatory synapses, which can lead to adaptation or differentiation (Tripp and Eliasmith 2010). In sum, in response to the sudden onset of a constant stimulus, the addition of rate adaptation to the model leads to an increased mean response with a slowing of intrinsic oscillations.

More interesting is the effect of rate adaptation when a slow oscillatory stimulus is added, in this case a 0.3 Hz sine wave (amplitude 100 Hz). Without the added rate adaptation, the intrinsic oscillation of 10 Hz can be seen superimposed on the 0.3 Hz of the input stimulus (Fig. 6a, blue trace). With the added adaptation time scales, the faster frequencies are slowed and the 0.3 Hz stimulus frequency is accentuated, especially in the case of the approximate power law adaptation (Fig. 6a, red trace; Fig. 6b, bottom panel). The power spectrum of the standard model shows distinct peaks at 0.3 Hz and ~10 Hz from the stimulus and intrinsic network properties, respectively (Fig. 6b, top panel). However, with the added adaptation, frequencies are blurred, slower frequencies have relatively more power, and frequencies intrinsic to the network become less obvious (Fig. 6b, middle and bottom panels). Thus, the high-pass filtering characteristics of rate adaptation added to one neural population of the network effectively yields an increase in low frequency power for the network output. Note that flattening of the power spectrum is more pronounced for the network incorporating adaptation with three time scales as compared to mono-exponential adaptation. This illustrates the potential importance of considering multiple time scale adaptation when simulating neural responses.

4 Discussion

Although rate adaption has long been noted (Adrian and Zotterman 1926) and is present in many neurons, both excitatory and inhibitory, its computational properties generally remain enigmatic (Wark et al. 2007). Rate adaptation often appears to have multiple time scales (La Camera et al. 2006) and multiple neuron types have been found to exhibit slow rate adaptation, including fast-spiking (Descalzo et al. 2005) and subthalamic neurons (Barraza et al. 2009) in addition to

Fig. 6 **a** Pyramidal neuron post-synaptic membrane potential ($y_1 - y_2$) in response to a 0.3 Hz sine wave stimulus with amplitude 100 Hz. Potentials have been low-pass filtered in the lower panel for illustrative purposes. Models without spike frequency adaptation (SFA), with single time scale adaptation ($\tau = 1$ s), and with multiple time scale adaptation ($\tau = [0.3\ 1\ 6]$ s) are represented by *blue*, *green*, and *red* traces, respectively. **b** Power spectra showing the contributions of output frequencies to the overall model output, where approximate power law adaptation shows the flattest power spectrum (*bottom panel*)
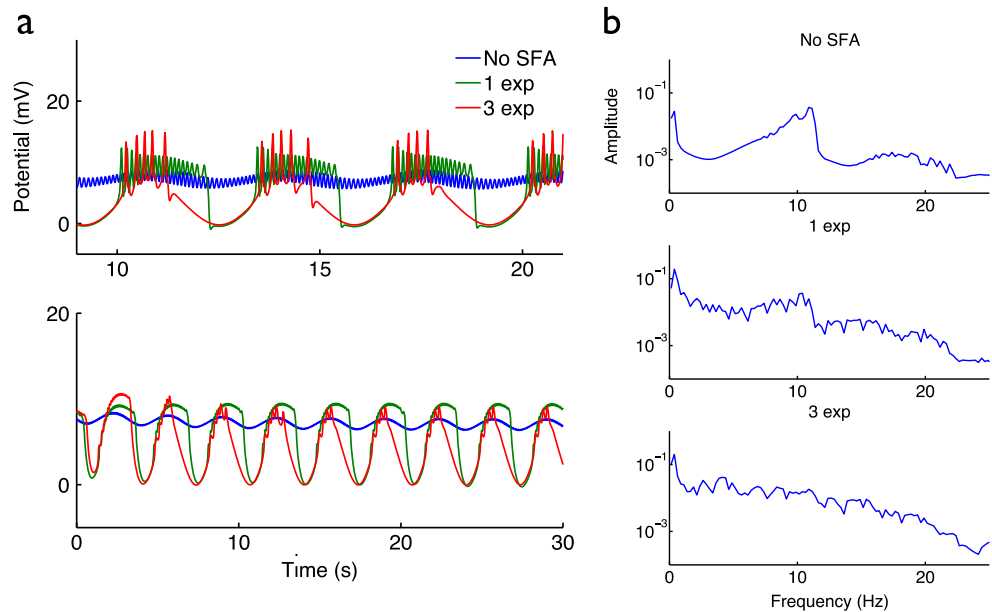
cortical neurons (Schwindt et al. 1988). Yet, multiple time scale adaptation is often not modeled in neural networks. Here, a straightforward method to incorporate multiple time scale adaptation into simplified neural networks is presented. Demonstrated in a model of local field potentials, the addition of rate adaptation facilitated the effect slowly oscillating stimuli on the network output and reduced the effect of intrinsic network frequencies.

It is clear from prior work that rate adaptation can be viewed as a linear filter on the stimulus, such as a first order linear filter that has high-pass characteristics (Benda and Herz 2003), a second order filter with band-pass characteristics (Shriki et al. 2003), or a power law filter (Lundstrom et al. 2008a). However, in none of these cases could arbitrary multiple time scale dynamics be modeled in a straightforward manner. Here, power law adaptation was approximated by filters with a physiological correspondence. The three time scales of the exponential filters were chosen to be $\tau = [0.3\ 1\ 6]$ s such that they roughly correspond to the medium after-hyperpolarization (AHP), early slow AHP, and late slow AHP currents, respectively (Madison and Nicoll 1984, Schwindt et al. 1988, Fleidervish et al. 1996, Abel et al. 2004). The fitted parameters then provide the weights for these currents, which correspond to relative channel conductances. Thus, given a measurement of the dynamics of rate adaptation, such as by assessing phase leads, and an estimate of the relevant time constants, this method suggests a relative weighting of channel conductances for the adaptation currents.

Mechanistically, adding cell intrinsic rate adaptation to the Jansen and Rit model in the presence of a slow 0.3 Hz oscillatory stimulus leads to a bursting-like output. As shown in detail previously for spiking neurons (Izhikevich 2007), at a

fundamental level bursting requires a slow modulating influence that interacts with a faster oscillating system. In this network even without added noise, the slow rate adaptation continually changes the dynamics of the faster oscillating system, thereby leading to an increased variety of output frequencies, and flattening the model's power spectrum (Fig. 6b). The addition of noise to the system would be expected to further broaden the distribution of output frequencies (Lundstrom et al. 2009). Power law adaption has been suggested to function as a means of temporal decorrelation that could promote efficiency of information transmission (Wark et al. 2007, Lundstrom et al. 2008a, Pozzorini et al. 2013). In this case, one immediate effect is that rate adaptation decreases the contribution of faster intrinsic oscillation frequencies to the output power spectrum, and increases the relative contribution of slower stimulus frequencies. This suggests that rate adaptation may have a physiological role in reducing the effect that the details of synaptic filtering have on the output frequencies of networks.

The potential role of rate adaptation in temporal decorrelation and dampening of intrinsic oscillations is intriguing. Infra-slow oscillations (ISOs) of ~0.01–0.2 Hz have been correlated with interictal epileptiform discharges on human electroencephalography (Vanhatalo et al. 2004), which are characterized by excessive, synchronous firing of distributed populations of neurons. ISOs have also been associated with successful human stimulus detection (Monto et al. 2008). Rate adaptation may be a mechanism to prevent excessive synchrony at intrinsic frequencies while promoting efficient information transmission via temporal decorrelation (Wark et al. 2007, Lundstrom et al. 2008a, Pozzorini et al. 2013). In general, given the prevalence of rate adaptation in healthy cortex, the fact that anti-epileptic drugs such as lacosamide

appear to promote rate adaptation (de Biase et al. 2014), and the association between ISOs and epileptic activity (Vanhatalo et al. 2004), rate adaptation may provide a compensatory response of cortex to epileptic activity. Methods for understanding and assessing rate adaptation may have significant clinical relevance.

The intent here has been to focus on multiple time scale rate adaptation as it affects neural rate responses on the ~1 Hz time scale and slower. Understanding rate adaptation as a process of stimulus filtering highlights rate adaptation as a history-dependent stimulus weighting and allows for a straightforward implementation in networks. Using this general adaptation filter model, each exponential filter potentially reflects the contribution of a specific biophysical channel conductance. While the focus here is on adaptation related to spike generation, evidence suggests that at least in some cases synaptic depression can be similarly characterized and has similar computational properties such that synaptic depression is analogous to spike rate adaptation (Puccini et al. 2007, Tripp and Eliasmith 2010). In conclusion, the goal of this approach is to facilitate network modeling that considers differing time scales of rate adaptation in order to further a deeper understanding of how adaptation time scales affect computation. These results suggest that rate adaptation may play an important role in network dynamics.

Appendix

Linear rate models with exponential rate adaptation

Rate models are often of the form $r = f(x-a)$, where f is some function of the input x with a feedback current a that depends on the firing rate r via some equation $a(r)$ describing adaptation dynamics (Benda and Herz 2003, La Camera et al. 2004). In one of the simplest such models the firing rate is a linear function of the stimulus and the negative feedback adaptation. The firing rate increases linearly with increasing stimulus, while the adaptation variable decays exponentially with time:

$$
\begin{aligned}
r &= mx - ga \\
\frac{da}{dt} &= \frac{-a}{\tau} + kr
\end{aligned}
\tag{13}
$$

where r is the firing rate, x is the time-varying stimulus, a is the adaptation variable, τ is the relaxation time constant, and

m, g, and k are gain constants. One way to see that this is a high pass system is to express the rate dependence in terms of only the stimulus, thus eliminating the adaptation variable a, and then examine the equation in the frequency domain. Expressing $r(t)$ as only a function of $x(t)$:

$$
\begin{aligned}
\frac{d}{dt}\left[\frac{m}{g}x - \frac{r}{g}\right] &= \frac{-1}{\tau}\left[\frac{mx}{g} - \frac{r}{g}\right] + kr \\
\frac{dr}{dt} &= -r\left(\frac{1}{\tau} + gk\right) + \frac{m}{\tau}x + m\frac{dx}{dt}
\end{aligned}
\tag{14}
$$

With $\tau_{eff} = (1/\tau + gk)^{-1}$ this becomes:

$$
\tau_{eff}\frac{dr}{dt} = -r + m\left(1 - gk\tau_{eff}\right)x + m\tau_{eff}\frac{dx}{dt}
\tag{15}
$$

which gives in the frequency domain:

$$
R = m\left(\frac{1 - gk\tau_{eff} + i\omega\tau_{eff}}{1 + i\omega\tau_{eff}}\right)X = m\left(1 - \frac{gk\tau_{eff}}{1 + i\omega\tau_{eff}}\right)X
\tag{16}
$$

and in the time domain:

$$
r(t) = m\left(x(t) - gkx(t) * e^{-t/\tau_{eff}}\right)
\tag{17}
$$

where $0 \leq gk\tau_{eff} \leq 1$. When $gk\tau_{eff} = 1$, it is clear that the system is that of adapting high pass filtering. In fact, as $gk\tau_{eff}$ increases, the amount of adaptation increases and the response to a step increase reflects a decay time course that is increasingly exponential-like. Notice that $\tau_{eff} \leq \tau$, as has been previously shown (Ermentrout 1998, Wang 1998, Tripp and Eliasmith 2010). The transfer function of Eq. (16) is identical to that derived in Benda and Herz (see Eq 5.8, 2003), where the gain parameters were expressed as slopes of the firing rate-input curve. The filter is:

$$
H(\omega) = m\frac{m_{ss}/m + i\omega\tau_{eff}}{1 + i\omega\tau_{eff}}
\tag{18}
$$

where m and m_{SS} are the slopes of the firing rate-input curve at an initial unadapted time and an adapted steady state, respectively. Here, $m_{SS} = m(1 - gk\tau_{eff})$ and since $\tau_{eff} = (1/\tau + gk)^{-1}$ one can see that $\tau_{eff} = \tau\, m_{SS}/m$. The degree of negative feedback provided by adaptation is expressed in the reduction of τ_{eff} from τ: the more adaptation the smaller τ_{eff}. Thus, the model of Eq. (16) is functionally equivalent to the universal exponential adaptation model derived in Benda and Herz (2003) from a standard spike-generating model of membrane potential and

currents. Here, linear dynamics were assumed initially rather than as an approximation during the derivation. By claiming the adaptation variable a can be described as a function of the firing rate r, rather than of individual spikes, one is assuming that τ is much greater than $1/r$. In order to separate the fast spike generator from slow adaptation, one assumes that fluctuations in a do not markedly affect the time course of the spike generator (Benda and Herz 2003).

Linear rate models with power law rate adaptation

One notable function that can be approximated by exponentials is the power law. This unique function has the special property of being scale invariant such that its shape is unchanged despite scaling the x-axis. In other words, power laws do not have a characteristic time scale. Adaptation in neocortical neurons has been found to perform a function that can be approximated by power law filters (Lundstrom et al. 2008a, Lundstrom et al. 2010). Power laws can be approximated by an infinite sum of exponentials as can be seen by using the definition of the gamma function (Thorson and Biederman-Thorson 1974, Fairhall and Bialek 2002):

$$\Gamma(k) \equiv \int_0^\infty \lambda^{k-1} e^{-\lambda} d\lambda.$$

Further, the Fourier transform of a power law is obtained by using the gamma function and setting $\lambda = i\omega t$ and $d\lambda = i\omega\, dt$:

$$(i\omega)^{-k} = \frac{1}{\Gamma(k)} \int_0^\infty t^{k-1} e^{-i\omega t} dt$$

Thus, by using the definition of the Fourier transform, the Fourier transform of a power law is:

$$(i\omega)^\alpha \xleftrightarrow{F} kt^{-(\alpha+1)} \tag{19}$$

where in the time domain $t \leq 0 = 0$. Experimentally, $(i\omega)^\alpha$ is a reasonable filter that describes the effect of adaptation on the stimulus (Lundstrom et al. 2008a, Lundstrom et al. 2010) with a model of adaptation as follows, shown below in the frequency domain:

$$R(\omega) = k(i\omega)^\alpha X(\omega) + b \tag{20}$$

where k and b are constants and α describes degree of adaptation. In the time domain, the equivalent filter for

$H(\omega) = i\omega^\alpha$ with a finite number of frequencies can be expressed as

$$h(t) = \frac{1}{\Gamma(1-\alpha)} \frac{d}{dt} \int_0^t (t-\tau)^{-\alpha} \frac{\sin nt}{\pi t} d\tau, \quad (0 \leq \alpha < 1)$$

where the following approximation for the delta function with finite range of frequencies is used (Arfken and Weber 1995):

$$\delta_n(t) = \frac{\sin nt}{\pi t} = \frac{1}{2\pi} \int_{-n}^n \exp(iwt) dw.$$

However, this form of the filter is difficult to use. An easier-to-use filter can be found by using the approach described above, where resulting dynamics are such that either the adaptation variable or the response to a step impulse has the form of a power law. For example, assuming power law dynamics of the adaptation variable with $h(t) = kt^{-\alpha}$, the appropriate model would be:

$$r(t) = mx(t) - mk \int x(\tau)(t-\tau)^{-\alpha} d\tau + b \tag{21}$$

with rate reponse r to a time-varying stimulus x with constants m, b, and k, with α controlling the degree of adaptation. Alternately, if a model that has precisely a power law decay of power α to a step increase is desired, the derivative of the power law yields the result:

$$r(t) = -m \int x(\tau)(t-\tau)^{-\alpha-1} d\tau + b \tag{22}$$

with constants m and b and α controlling the degree of adaptation, as displayed in Fig. 7. Practically, discrete time power law filters as in Eqs. (21) and (22) are limited approximations for the frequency domain filter of $(i\omega)^\alpha$. They are not defined at time zero, and thus the initial response to a stimulus, which should not be dependent on any adaptation dynamics, may be discontinuous with the subsequent decay. In addition, a power law has an infinitely long tail, which can only be approximated by a finite length filter.

The relationship between magnitude and phase in minimum phase systems

Typically there is no precise relationship between the frequency-response magnitude, or gain, for a linear time invariant system and its phase. However, for systems characterized by a rational response function there is a relationship and for a subset of rational systems termed minimum phase systems, specifying the phase determines the magnitude to within

a

b
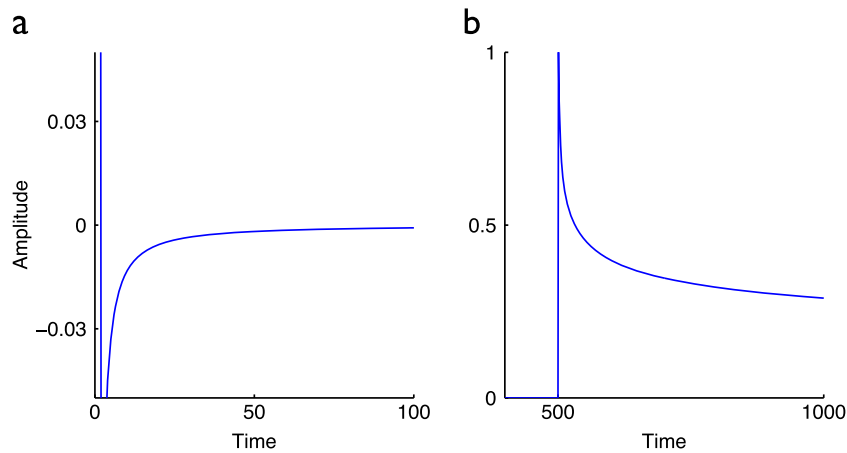
Fig. 7 a A power law filter h with $\alpha = 0.2$, according to Eq (22). The magnitude of the filter was normalized such that its first point was equal to 1, which is not displayed for convenience. **b** The response of h convolved with a step function. Note that the initial peak response is determined by the arbitrary first point of the filter. The power law does not have a defined steady state, and thus eventually decays to zero given an infinite filter length, in contrast to an exponential filter which decays to some steady state

a single scale factor, and vice versa (Oppenheim et al. 1999). A rational LTI system that is causal, stable, and that in the Laplace domain has all zeros on the left side of the s-plane (or inside the unit circle of the z-plane for the z-transform) is a minimum phase system (Ulrych and Lasserre 1966, Oppenheim et al. 1999). Causality assumes that the filter is right-sided, that is, it is equal to zero for negative time points, meaning that the output cannot precede the input. Stability implies a bounded output sequence for every bounded input sequence, which suggests that the discrete time impulse response is absolutely summable:

$$\sum_{n=-\infty}^{\infty} |h[n]| < \infty \tag{23}$$

The last requirement for a minimum phase system, which amounts to assuming that the inverse system H is also causal and stable, is equivalent to requiring all τ_n in the adaptation filter models to be nonnegative. Specifically, in the Laplace domain Eq. (10) has a numerator of the form:

$$(1/\tau_1 + s)(1/\tau_2 + s)...(1/\tau_n + s) \tag{24}$$

where zeros can be seen to be negative, that is, on the left side of the s-plane, as long as all τ_n are nonnegative. This implies that the magnitude and phase of the system are related through the Hilbert transfrom (Ulrych and Lasserre 1966, Oppenheim et al. 1999):

$$\angle H(\omega) = -\frac{1}{\pi} PV \int_{-\infty}^{\infty} \frac{\log|H(x)|}{\omega - x} dx \tag{25}$$

where $\angle H(\omega)$ is the phase and PV signfies the principal value of the Cauchy integral of the Hilbert transform. The Hilbert transform can be understood as convolving a function with the filter $1/(\pi x)$, where the function in this case is the logarithm of the magnitude of $H(\omega)$. Approaching negative and positive infinity as values approach zero from the negative and positive side, respectively, $1/x$ is effectively a differentiating filter. Thus, from Eq. (25) the phase is related to the derivative of the magnitude. The phase is positive for high pass filters, meaning that rate adaptation gives rise to phase leads.

Implementing the Jansen and Rit model of EEG oscillations

The standard Jansen and Rit model (Jansen and Rit 1995) specified as a system differential equations was implemented with a fourth order Runge Kutta solver as:

$$y_1' = y_4$$

$$y_2' = y_5$$

$$y_3' = y_6$$

$$y_4' = k_e/\tau_e(S + c_2 Sgm(c_1 y_3)) - 2/\tau_e y_4 - 1/\tau_e^2 y_1$$

$$y_5' = k_i/\tau_i c_4 Sgm(c_3 y_3) - 2/\tau_i y_5 - 1/\tau_i^2 y_2$$

$$y_6' = k_e/\tau_e Sgm(y_1 - y_2) - 2/\tau_e y_6 - 1/\tau_e^2 y_3$$

with sigmoid $Sgm(v) = e_0/[1 + exp(0.56(6 - v))$, external stimulus ($S$), constants $c_{1-4} = [135\ 108\ 33.75\ 33.75]$, and parameters $k_e = 3.25$mV, $k_i = 22$mV, $\tau_e = 10$ms, $\tau_i = 20$ms, and $e_0 = 5$ Hz, unless otherwise noted. Primes indicate temporal first-order derivatives. ODEs were solved by a fourth-order fixed step Runge Kutta solver with $dt = 1$–5ms, with identical

results obtained regardless. The stimulus was either constant or a sine wave. To stimulate rate adaptation with three time scales, the following system was implemented:

$$y_1' = y_4$$

$$y_2' = y_5$$

$$y_3' = y_6$$

$$y_4' = y_{10}$$

$$y_5' = y_{11}$$

$$y_6' = k_e/\tau_e Sgm(y_7) - 2/\tau_e y_6 - 1/\tau_e^2 y_3$$

$$y_7' = y_8$$

$$y_8' = y_9$$

$$y_9' = (y_{10}' - y_{11}') + k_1(y_{10} - y_{11}) + k_2(y_4 - y_5)$$
$$+ k_3(y_1 - y_2) - k_4 y_9 - k_5 y_8 - k_6 y_7$$

$$y_{10}' = k_e/\tau_e \left(S' + c_1 c_2 y_6 Sgm'(c_1 y_3) - 2/\tau_e y_{10} - /\tau_e^2 y_4 \right)$$

$$y_{11}' = k_i/\tau_i c_3 c_4 y_6 Sgm'(c_3 y_3) - 2/\tau_i y_{11} - 1/\tau_i^2 y_5$$

with the following additional parameters:

$$k_1 = 1/\tau_1 + 1/\tau_2 + 1/\tau_3$$

$$k_2 = 1/(\tau_1 + \tau_2) + 1/(\tau_1 + \tau_3) + 1/(\tau_2 + \tau_3)$$

$$k_3 = 1/(\tau_1 \tau_2 \tau_3)$$

$$k_4 = k_1 = kg_1 + kg_2 + kg_3$$

$$k_5 = k_2 + kg_1/(\tau_2 + \tau_3) + kg_2(\tau_1 + \tau_3)$$
$$+ kg_3/(\tau_1 + \tau_2)$$

$$k_6 = k_3 + kg_1/(\tau_2 \tau_3) + kg_2(\tau_1 \tau_3) + kg_3/(\tau_1 \tau_2)$$

where kg_n and τ_n as parameters governing the gain and time constant of each exponential filter. Similar smaller systems of ODEs were simulated for the cases with one or two exponential filters with identical results as those obtained by setting the

appropriate gain parameters to zero above. This model can also be simulated with the corresponding filter or integral equations rather than the above differential equations. The overall output of the model is the difference between the post-synaptic excitatory and inhibitory membrane potentials to the pyramidal neurons ($y_1 - y_2$), consistent with what is thought to primarily underlie the signal of electroencephalography (Nunez and Srinivasan 2006).

References

Abel, H. J., Lee, J. C., Callaway, J. C., & Foehring, R. C. (2004). Relationships between intracellular calcium and afterhyperpolarizations in neocortical pyramidal neurons. *Journal of Neurophysiology, 91*, 324–335.

Adrian, E. D., & Zotterman, Y. (1926). The impulses produced by sensory nerve endings: part 2. The response of a single End-organ. *The Journal of Physiology, 61*, 151–171.

Arfken, G. B., & Weber, H.-J. (1995). *Mathematical methods for physicists*. San Diego: Academic.

Barlow, HB. (1961) Possible principles underlying the transformation of sensory messages. In: Sensory communication. In W Rosenblith(ed.), MIT Press.

Barraza, D., Kita, H., & Wilson, C. J. (2009). Slow spike frequency adaptation in neurons of the rat subthalamic nucleus. *Journal of Neurophysiology, 102*, 3689–3697.

Benda, J., & Herz, A. V. (2003). A universal model for spike-frequency adaptation. *Neural Computation, 15*, 2523–2564.

Brenner, N., de Ruyter, B. W., & van Steveninck, R. (2000). Adaptive rescaling maximizes information transmission. *Neuron, 26*, 695–702.

Compte, A., Sanchez-Vives, M. V., McCormick, D. A., & Wang, X. J. (2003). Cellular and network mechanisms of slow oscillatory activity (<1 Hz) and wave propagations in a cortical network model. *Journal of Neurophysiology, 89*, 2707–2725.

Connor, J. A., & Stevens, C. F. (1971). Prediction of repetitive firing behaviour from voltage clamp data on an isolated neurone soma. *The Journal of Physiology, 213*, 31–53.

David, O., & Friston, K. J. (2003). A neural mass model for MEG/EEG: coupling and neuronal dynamics. *NeuroImage, 20*, 1743–1755.

Dayan, P., & Abbott, L. F. (2001). *Theoretical neuroscience: computational and mathematical modeling of neural systems*. Cambridge: Massachusetts Institute of Technology Press.

de Biase, S., Gigli, G. L., Valente, M., & Merlino, G. (2014). Lacosamide for the treatment of epilepsy. *Expert Opinion on Drug Metabolism & Toxicology, 10*, 459–468.

Deco, G., Jirsa, V. K., Robinson, P. A., Breakspear, M., & Friston, K. (2008). The dynamic brain: from spiking neurons to neural masses and cortical fields. *PLoS Computational Biology, 4*, e1000092.

Demanuele, C., Broyd, S. J., Sonuga-Barke, E. J., & James, C. (2013). Neuronal oscillations in the EEG under varying cognitive load: a comparative study between slow waves and faster oscillations. *Clinical Neurophysiology: Official Journal of the International Federation of Clinical Neurophysiology, 124*, 247–262.

Descalzo, V. F., Nowak, L. G., Brumberg, J. C., McCormick, D. A., & Sanchez-Vives, M. V. (2005). Slow adaptation in fast-spiking neurons of visual cortex. *Journal of Neurophysiology, 93*, 1111–1118.

Destexhe, A., Hughes, S. W., Rudolph, M., & Crunelli, V. (2007). Are corticothalamic 'up' states fragments of wakefulness? *Trends in Neurosciences, 30*, 334–342.

Drew, P. J., & Abbott, L. F. (2006). Models and properties of power-law adaptation in neural systems. *Journal of Neurophysiology, 96*, 826–833.

Ermentrout, B. (1998). Linearization of F-I curves by adaptation. *Neural Computation, 10*, 1721–1729.

Ermentrout, G. B., & Cowan, J. D. (1979). Temporal oscillations in neuronal nets. *Journal of Mathematical Biology, 7*, 265–280.

Fairhall A, Bialek, W. (2002) Adaptive spike coding. In: The Handbook of Brain Theory and Neural Networks. In M. Arbib (ed.), MIT Press.

Fairhall, A. L., Lewen, G. D., de Ruyter, B. W., & van Stevenick, R. (2001a). Multiple timescales of adaptation in a neural code. In T. K. Leen (Ed.), *Advances in Neural Information Processing Systems 13* (pp. 124–130). Cambridge: MIT Press.

Fairhall, A. L., Lewen, G. D., Bialek, W., & de Ruyter Van Stevenick, R. R. (2001b). Efficiency and ambiguity in an adaptive neural code. *Nature, 412*, 787–792.

Fellous, J. M., & Sejnowski, T. J. (2000). Cholinergic induction of oscillations in the hippocampal slice in the slow (0.5–2 Hz), theta (5–12 Hz), and gamma (35–70 Hz) bands. *Hippocampus, 10*, 187–197.

Fleidervish, I. A., Friedman, A., & Gutnick, M. J. (1996). Slow inactivation of Na+current and slow cumulative spike adaptation in mouse and guinea-pig neocortical neurones in slices. *The Journal of Physiology, 493*(Pt 1), 83–97.

Gerstner, W., & Kistler, W. M. (2002). *Spiking neuron models : single neurons, populations, plasticity*. Cambridge: Cambridge University Press.

Harris, J., & Stöcker, H. (1998). *Handbook of mathematics and computational science*. New York: Springer.

Higgs, M. H., Slee, S. J., & Spain, W. J. (2006). Diversity of gain modulation by noise in neocortical neurons: regulation by the slow afterhyperpolarization conductance. *The Journal of Neuroscience, 26*, 8787–8799.

Hodgkin, A. L., & Huxley, A. F. (1952). A quantitative description of membrane current and its application to conduction and excitation in nerve. *Journal of Physiology, 117*, 500–544.

Izhikevich, E. M. (2007). *Dynamical systems in neuroscience: the geometry of excitability and bursting*. Cambridge: MIT Press.

Jansen, B., & Rit, V. (1995). Electroencephalogram and visual evoked potential generation in a mathematical model of coupled cortical columns. *Biological Cybernetics, 73*, 357–366.

Koch, C. (1999). *Biophysics of computation: information processing in single neurons*. New York: Oxford University Press.

La Camera, G., Rauch, A., Luscher, H. R., Senn, W., & Fusi, S. (2004). Minimal models of adapted neuronal response to *in vivo*-like input currents. *Neural Computation, 16*, 2101–2124.

La Camera, G., Rauch, A., Thurbon, D., Luscher, H. R., Senn, W., & Fusi, S. (2006). Multiple time scales of temporal response in pyramidal and fast spiking cortical neurons. *Journal of Neurophysiology, 96*(6), 3448–64.

Liu, Y. H., & Wang, X. J. (2001). Spike-frequency adaptation of a generalized leaky integrate-and-fire model neuron. *Journal of Computational Neuroscience, 10*, 25–45.

Lundqvist, M., Herman, P., Palva, M., Palva, S., Silverstein, D., & Lansner, A. (2013). Stimulus detection rate and latency, firing rates and 1-40Hz oscillatory power are modulated by infra-slow fluctuations in a bistable attractor network model. *NeuroImage, 83*, 458–471.

Lundstrom, B. N., Higgs, M. H., Spain, W. J., & Fairhall, A. L. (2008). Fractional differentiation by neocortical pyramidal neurons. *Nature Neuroscience, 11*, 1335–1342.

Lundstrom. BN., Hong, S., Higgs, MH., Fairhall, AL. (2008b) Two Computational Regimes of a Single-Compartment Neuron Separated by a Planar Boundary in Conductance Space. *Neural Comput*

Lundstrom, B. N., Famulare, M., Sorensen, L. B., Spain, W. J., & Fairhall, A. L. (2009). Sensitivity of firing rate to input fluctuations depends on time scale separation between fast and slow variables in single neurons. *Journal of Computational Neuroscience, 27*, 277–290.

Lundstrom, B. N., Fairhall, A. L., & Maravall, M. (2010). Multiple timescale encoding of slowly varying whisker stimulus envelope in cortical and thalamic neurons *in vivo*. *The Journal of Neuroscience, 30*, 5071–5077.

Madison, D. V., & Nicoll, R. A. (1984). Control of the repetitive discharge of rat CA 1 pyramidal neurones *in vitro*. *The Journal of Physiology, 354*, 319–331.

Monto, S., Palva, S., Voipio, J., & Palva, J. M. (2008). Very slow EEG fluctuations predict the dynamics of stimulus detection and oscillation amplitudes in humans. *The Journal of Neuroscience, 28*, 8268–8272.

Moran, R., Pinotsis, D. A., & Friston, K. (2013). Neural masses and fields in dynamic causal modeling. *Frontiers in Computational Neuroscience, 7*, 57.

Nunez, P. L., & Srinivasan, R. (2006). *Electric fields of the brain : the neurophysics of EEG*. Oxford: Oxford University Press.

Oppenheim, A. V., Schafer, R. W., & Buck, J. R. (1999). *Discrete-time signal processing*. Upper Saddle River: Prentice Hall.

Pozzorini, C., Naud, R., Mensi, S., & Gerstner, W. (2013). Temporal whitening by power-law adaptation in neocortical neurons. *Nature Neuroscience, 16*, 942–948.

Puccini, G. D., Sanchez-Vives, M. V., & Compte, A. (2007). Integrated mechanisms of anticipation and rate-of-change computations in cortical circuits. *PLoS Computational Biology, 3*, e82.

Sanchez-Vives, M. V., Nowak, L. G., & McCormick, D. A. (2000). Cellular mechanisms of long-lasting adaptation in visual cortical neurons *in vitro*. *The Journal of Neuroscience, 20*, 4286–4299.

Schwindt, P. C., Spain, W. J., Foehring, R. C., Chubb, M. C., & Crill, W. E. (1988). Slow conductances in neurons from cat sensorimotor cortex *in vitro* and their role in slow excitability changes. *Journal of Neurophysiology, 59*, 450–467.

Shriki, O., Hansel, D., & Sompolinsky, H. (2003). Rate models for conductance-based cortical neuronal networks. *Neural Computation, 15*, 1809–1841.

Steriade, M. (2006). Grouping of brain rhythms in corticothalamic systems. *Neuroscience, 137*, 1087–1106.

Steriade, M., Contreras, D., Curro Dossi, R., & Nunez, A. (1993). The slow (<1 Hz) oscillation in reticular thalamic and thalamocortical neurons: scenario of sleep rhythm generation in interacting thalamic and neocortical networks. *The Journal of Neuroscience, 13*, 3284–3299.

Thorson, J., & Biederman-Thorson, M. (1974). Distributed relaxation processes in sensory adaptation. *Science, 183*, 161–172.

Trappenberg, T. P. (2002). *Fundamentals of Computational Neuroscience*. USA: Oxford University Press.

Tripp, B. P., & Eliasmith, C. (2010). Population models of temporal differentiation. *Neural Computation, 22*, 621–659.

Ulrych, T., & Lasserre, M. (1966). Minimum-phase. *Canadian Journal of Exploration Geophysics, 2*, 22–32.

Vanhatalo, S., Palva, J. M., Holmes, M. D., Miller, J. W., Voipio, J., & Kaila, K. (2004). Infraslow oscillations modulate excitability and interictal epileptic activity in the human cortex during sleep. *Proceedings of the National Academy of Sciences of the United States of America, 101*, 5053–5057.

Vinagre, B., Podlubny, I., Hernandez, A., & Feliu, V. (2000). Some approximations of fractional order operators used in control theory

and applications. *Fractional Calculus and Applied Analysis, 3*, 231–248.

Wang, X. J. (1998). Calcium coding and adaptive temporal computation in cortical pyramidal neurons. *Journal of Neurophysiology, 79*, 1549–1566.

Wark, B., Lundstrom, B. N., & Fairhall, A. (2007). Sensory adaptation. *Current Opinion in Neurobiology, 17*, 423–429.

Wendling, F., Bellanger, J. J., Bartolomei, F., & Chauvel, P. (2000). Relevance of nonlinear lumped-parameter models in the analysis of depth-EEG epileptic signals. *Biological Cybernetics, 83*, 367–378.